January 2012

Golgi & Eres Biogenesis In The Malaria-Causing Parasite Plasmodium Falciparum

Michelle Morales

Golgi & ERES Biogenesis in the Malaria-Causing Parasite *Plasmodium falciparum*

A Thesis Submitted to the
Yale University School of Medicine
in Partial Fulfillment of the Requirements for the
Degree of Doctor of Medicine

Michelle Morales
2012

Golgi & ERES Biogenesis in the Malaria-Causing Parasite *Plasmodium falciparum*

Michelle Morales, Susann Herrmann and Tim-Wolf Gilberger, Bernhard Nocht Institute for Tropical Medicine, Hamburg, Germany. Sponsored by Choukri Ben Mamoun, Department of Internal Medicine, Yale University School of Medicine, New Haven, CT.

Plasmodium falciparum, the parasite causing the most severe form of human malaria, continues to bear a global burden of morbidity and mortality. No vaccine is available and resistance is emerging and expanding to all classes of existing antimalarials. Relatively little is known about the secretory pathway of *P. falciparum*, which has the ability to export proteins to specialized parasite organelles and into the host erythrocyte to create the ideal environment for growth.

This thesis is focused on an understanding of the biogenesis of two critical organelles within *P. falciparum*'s secretory pathway: endoplasmic reticulum exit sites (ERES) and the Golgi apparatus. This study cloned parasites containing fluorescently-labeled proteins to identify ERES (Sec13p) and the Golgi apparatus (GRASP). Time lapse 3D microscopy, photobleaching and photoconversions were used to visualize the process.

In this thesis, it was shown that *Plasmodium falciparum* ERES undergo recruitment at rapid rates of approximately 15.2 seconds following photobleaching experiments. Evidence gathered via time-lapse microscopy in conjunction with photoconversions of Sec13p fused to Dendra showed that ERES form de novo. Although conclusive evidence on Golgi biogenesis was not obtained, given the close spatial and duplication time relationship between ERES and the Golgi and previous studies in *Pichia pastoris* and *Trypanosoma brucei*, it is speculated that the Golgi similarly forms de novo. Strides were made towards the creation of a GRASP knock-out and examination of GRASP interaction partners in *P. falciparum*, which after optimization of methods, may allow for a more detailed study of Golgi biogenesis, GRASP affect on Golgi architecture and on alternative secretion of proteins. It is hoped these conclusions will further the understanding of the *P. falciparum* secretory pathway, which may ultimately lead to novel drug targets in the fight against malaria.

Acknowledgements

I would like to thank Tim-Wolf Gilberger for offering me a position in his lab and being an excellent mentor from any corner of the globe. Choukri Ben Mamoun for being a patient and supportive thesis advisor. Thomas Braulke for allowing me to join the Graduate College GRK1459 at the University of Hamburg Medical Center.

All the members of the Gilberger lab and the neighboring Spielmann lab for their help, advice and friendship: Boris Prinz, Ulrike Ruch, Sven Flemming, Florian Kruse, Alexander Oberli, Maya Kono, Arlett Heiber, Dipto Sinha, Susi Herrmann and especially Christof Grüring for teaching me confocal microscopy techniques.

My family and friends in the US for always being there in spirit. My new friends in Germany for being patient while I learned the language and for making this experience unforgettable. Johannes Keller for making Hamburg my home. And my medical student colleagues in Uganda for showing me the true human toll of malaria.

Table of Contents

Introduction

Malaria Past and Present

Malaria has been a global burden for centuries, possibly millenniums. Clay tablets in Mesopotamia dated to 2000 B.C. and Papyri in Egypt dated to 1570 B.C. contained references to what is almost certainly the disease[1]. The beginning of modern knowledge on malaria pathogenesis occurred about 130 years ago when Charles Louis Alphonse Laveran, a French physician stationed in a military hospital in Algeria, discovered parasites in the blood of a recently diseased malaria patient [2].

Since that time, disease patterns have significantly changed, in large part due to efforts toward prevention, eradication, detection and treatment. The World Health Organization (WHO) implemented the WHO Global Malaria Eradication Programme in 1955, spearheading the use of chloroquine for malaria prophylaxis and treatment plus dichlorodiphenyltrichloroethane (DDT) for vector control [3]. In part due to loss of political and financial support, the goal of global eradication was abandoned in the early 1970s; at the same time a surge of malaria cases in sub-Saharan Africa, exacerbated by chloroquine-resistant malaria and DDT-resistant *Anopheles* mosquito vectors, was noticed [3].

In spite of setbacks resulting from parasite and vector adaptation, promising trends in global recession have been observed. In 1900, it is estimated that 58% of the Earth's land surface was malaria endemic, compared with 30% in 2007; the decrease was mainly attributed to economic development and prevention strategies [4].

Nonetheless, sub-Saharan Africa is overwhelmed with malaria to this day, with temperatures and environmental factors playing a huge role in the existence of the disease. In temperate climates, the malarial reproduction rate is drastically lower than in the tropics, with malarial development ceasing all-together below 16 degrees Celsius [5]. Poverty complicates the situation, with poor housing providing inadequate protection from mosquitoes, prohibitive costs rendering insecticide-treated bed nets inaccessible and low levels of literacy and education leading to decreased knowledge of malaria prevention and symptom recognition [6]. The cycle worsens when you consider the high rate of malarial infection in pregnant women, partially secondary to decreased immunity in the gravid state. Malaria greatly increases the risk of delivering a low birth weight infant, who is known to have a significant risk of neuro-cognitive delay, with a two-to-four fold increased likelihood of failing school [5].

The World Malaria Report 2010 reported an estimated 225 million cases of malaria worldwide in 2009, down from 244 million in 2005 [7]. The biggest decrease in incidence during the four year period occurred in Europe and the Americas. Africa carried the burden of the disease, with 78% of cases and 91% of deaths [7]. There was also a decline in worldwide malarial deaths from 985,000 in 2000 to 781,000 in 2009, but 85% of these deaths occurred in one of the most vulnerable sections of society, children under five years of age [7].

Plasmodium Variations

The eukaryotic genus *Plasmodium* is responsible for malaria, a mosquito-borne disease.

Plasmodium is a member of the phylum Apicomplexa, a large group of approximately five thousand obligate intracellular protozoan parasites that also includes the human-disease causing organisms *Cryptosporidium*, *Babesia* and *Toxoplasma* [8]. Many species of *Plasmodium* have been characterized, including several strains recently discovered in African apes – one of which is believed to be the immediate precursor to *Plasmodium falciparum* [9]. However, only four species are known to routinely infect humans; these include *Plasmodium falciparum*, *Plasmodium vivax*, *Plasmodium ovale* and *Plasmodium malariae* [10]. A fifth species, *Plasmodium knowlesi*, was previously believed to infect only long-tailed macaque monkeys, but has been shown to naturally infect humans in Southeast Asia, particularly Malaysia [11].

These species vary in pathogenesis and severity. *P. vivax* and *P. ovale* have the ability to form inactive hypnozoites which can remain dormant in the liver for months to years, although the existence of hypnozoites in *P. ovale* is now debated [3, 12]. The activation of dormant hypnozoites can lead to a relapse of malaria, making these species difficult to eradicate [13]. *P. vivax* can also lead to severe anemia (Hemoglobin less than 5g/dl), particularly in children, and lung injury from inflammatory increases in alveolar-capillary permeability [14, 15]. *P. malariae* does not form hypnozoites, but can persist for decades as an asymptomatic blood infection [3]. *P. falciparum* is the most virulent and deadly form, and the subject of this research. It has an ability to modify the surface of host red blood cells with knobs that can adhere to vascular endothelium, leading to occlusion in organs such as the brain (leading to cerebral malaria) or placenta (one in four women in Sub-Saharan Africa has evidence of placental infection at the time of delivery) [16, 17].

Plasmodium falciparum Life Cycle

During the blood meal of a female *Anopheles* mosquito, *Plasmodium* sporozoites can be injected into the human dermis and enter the blood stream. From there, sporozoites are carried to the liver and cross through liver macrophages, Kupffer cells, into hepatocytes [3]. In the hepatocytes, infective merozoites are formed via massive asexual replication. These hepatic merozoites reach the blood stream by inducing host cell death and detachment, while simultaneously inhibiting exposure of phosphatidlyserine (a phagocytic signal) on the host plasma membrane, thereby ensuring self-protection from host immunity [18].

Once blood-borne, *P. falciparum* merozoites can invade any erythrocyte. Invasion is a complicated process that begins with the recognition of red blood cell (RBC) surface receptors over a long distance. This is followed by reorientation of the parasite's apical end to the erythrocyte surface, formation of a tight junction with a high affinity ligand-receptor interaction, invasion of the erythrocyte by the parasite's actin-myosin motor, shedding of the parasite's surface coat by a serine protease with concurrent formation of a parasitophorous vacuole (a compartment that surrounds the parasite and allows further maturation), and finally resealing of the RBC membrane [19].

The invasion process was at the forefront of the search for a vaccine against malaria. Apical Membrane Antigen 1 (AMA-1), a micronemal protein of apicomplexan parasites that is believed to be essential for invasion, was a promising candidate, eliciting immune

responses that inhibited parasites in vitro and in animal models. Unfortunately, the polymorphic nature of the antigen greatly decreased vaccine efficacy in human trials [20].

Invasion begins the forty eight hour asexual life cycle. Upon invasion, the former merozoite is now termed ring stage. This ring-stage parasite lasts approximately twenty two hours. During the ring stage, host-cell remodeling, such as formation of knobs on the infected red blood cell (iRBC) surface for endothelial adhesion and formation of Maurer's clefts for protein trafficking, takes place [21, 22]. The parasite also begins ingesting hemoglobin for an energy source, creating haemozoin as a byproduct. The parasite then transitions to a trophozoite stage, during which growth continues and DNA replication begins. At 36 hours post-infection, the trophozoite matures to a schizont-stage parasite. This stage is characterized by nuclear division, leaving 8-32 new nuclei in the parasite. Cell division results in 32 mono-nucleated merozoites. The iRBC then bursts, releasing free merozoites into the blood stream to infect new erythrocytes [23]. This asexual life cycle is the cause of symptoms, such as cyclical fever, associated with malarial disease.

Some parasites in the asexual, blood-stage cycle develop into gametocytes, or sexual forms that can be taken up by female *Anopheles* mosquitoes during subsequent blood meals. Male and female gametocytes meet in the mosquito midgut, resulting in fertilization and subsequent development until new *P. falciparum* sporozoites are formed and reach the mosquito salivary gland, where they can be injected into human skin, repeating the infection cycle [3].

Secretory Pathway of Proteins

An endoplasmic reticulum (ER), endocytic organelles and a plasma membrane are features of all known eukaryotic cells. Although the conservation of secretory apparatus and protein targeting sequences can be traced as far back as amebae on the evolutionary tree[24], the emergence of such a system is generally considered to be a crucial stage in the transition from prokaryotic to eukaryotic organisms[25].

Within the secretory pathway, the ER is the site of translocation, integration, protein folding and modification, and phospholipid and steroid biosynthesis[26]; it is in close association with the cell nucleus[27]. The ER can be divided into three distinct regions: rough ER, smooth ER, and transitional ER. The rough ER is so named because of its texture, stemming from the presence of ribosomes in all cells synthesizing proteins[28]. The smooth ER is the site of lipid biosynthesis[29]. The transitional ER (also named ER exit sites, or ERES as used in this thesis) are sites of protein exit from the ER[30].

The ERES, characterized by the presence of COPII vesicle components, are regions that export proteins to the Golgi apparatus[31]. Cop II coated vesicles contain two protein complexes (Sec23p/Sec24p and Sec13p/Sec31p) and the GTPase Sar1p[32]. Recently, it has been shown that Sec13p ridigidfies the COPII vesicle and influences membrane bending[33]. The cytosolic components arrange themselves at ERES to transport cargo to the Golgi apparatus. Numerous components of COPII-mediated transport have been identified in *P. falciparum*, including Sec13p, used as an ERES marker[34]. ERES morphology has also been shown to have a relationship with the morphology of the Golgi apparatus. In *Pichia pastoris*, ERES are well defined and in close approximation with the cis-Golgi; the Golgi apparatus is a classically stacked structure in this organism[35]. In

contrast, *Saccharomyces cerevisae* demonstrates COPII vesicle components along the entire ER membrane; the Golgi in this organism is unstacked and scattered throughout the cytoplasm[35]. In *P. falciparum*, ERES (as visualized with the ERES marker Sec13p), are noted to be defined, restricted areas of the ER membrane in close association with the Golgi[36].

The Golgi apparatus is one of the most important organelles in the secretory pathway, functioning as a processing, sorting and protein modification center[26]. The Golgi is believed to undergo continuous remodeling, stemming from protein transport via ERES[37]. Golgi can vary widely in morphology between organisms[38], but generally consists of a cis-Golgi, medial region and trans-Golgi. The cis-Golgi acts as the docking site for COPII-coated vesicles containing proteins from ERES, as well as the site of COPI vesicle budding (important for retrograde transport from Golgi to ER), while the trans-Golgi is a major sorting station for the secretory pathway and the "crossroads of the endocytic and exocytic pathways" [39, 40].

P. falciparum lacks some protein modification abilities, in particular N glycosylation[41], but does possess a Golgi apparatus. The Golgi is not stacked, is singular early in the parasite life cycle and duplicates prior to nuclear division and continues to duplicate until each progeny has its own singular Golgi prior to the bursting of infected red blood cells and release of merozoites[42]. The Golgi also has distinct cis- and trans-Golgi in close connection, but spatially separated as parasite maturation occurs[36]. How the Golgi duplicates in *P. falciparum* has not been proven. In *Trypanosoma brucei*, the Golgi also begins as a singular entity early in the life cycle before a new Golgi emerges de novo and

in close proximity to the ERES[43, 44]. In contrast, Toxoplasma gondii performs Golgi duplication via lateral extension followed by medial fission[45].

Golgi Re-Assembly and Stacking Protein (GRASP)

The Golgi Re-Assembly and Stacking Proteins (GRASPs) were discovered over ten years ago as proteins anchored to the Golgi membrane which participate in membrane tethering events and provide structural support to Golgi architecture[46]. The proteins are found in most eukaryotes and are generally encoded as a single copy in genomes. In vertebrates, a gene duplication event led to two proteins, GRASP65 and GRASP55, varying in location (cis-Golgi for GRASP65 and medial Golgi for GRASP55), interaction partners and molecular weight[47]. Both proteins contain a highly conserved N-terminal domain, an N-terminal membrane attachment motif and a divergent C-terminus enriched in serine and proline[48]. This C-terminus is the site of phosphorylation leading to unstacking of the Golgi at mitosis followed by dephosphorylation leading to restacking; it also serves as a substrate for caspases during apoptosis[49].

Although GRASPs are believed to play a crucial role in the stacking of Golgi cisternae, it was not understood why some organisms possessing copies of GRASP do not have stacked Golgi. Interestingly, a GRASP knock-out in *Disctyostelium discoideum* did not have an effect on Golgi architecture, but did prevent transport of the protein AcbA[50, 51]. These findings raised questions of whether GRASP was involved in alternative secretion of proteins. The findings have been duplicated in the yeast *Pichia pastoris*, suggesting a pathway for alternative secretion may have been evolutionarily conserved[52].

In *P. falciparum*, GRASP (which is used to visualize the Golgi) posses a splice variant that leads to the expression of two GRASP isoforms, termed GRASP1 and GRASP2, located at the cis-Golgi. GRASP2 differs at its N-terminus, possessing a region similar to that of fungi GRASP[42]. Since *P. falciparum* does not have a stacked Golgi, but has two isoforms of GRASP, it has been postulated that GRASP is more important for alternative secretion in the parasite. P. falciparum generally utilizes a PEXEL (*Plasmodium falciparum* EXport ELement) motif consisting of the amino acids R/KxLxE/QD, where x represents any amino acid to mark proteins destined for export[53]. However, PEXEL-negative exported proteins, or PNEPs lacking the motif exist and the number identified continues to grow[54]. A link between PNEP export and GRASP may lead to understanding this alternate pathway.

Current Drug Options and Resistance

Current antimalarials work at different stages of the parasite life cycle, with nearly all having a method of action during the asexual blood stages[55]. Drugs currently available to treat malaria can be classified based on known methods of action. Nucleic acid inhibitors, including sulfonamides and sulfines in type 1 and pyrimethamines, trimethoprim and biguanides, such as proguanil, in type 2, act to inhibit the folate pathway, ultimately decreasing DNA synthesis[56]. These drugs are susceptible to mutations at binding sites. Napthoquinones, such as atovaquone, similarly inhibit nucleic acid formation, and have demonstrated resistance at conenzyme Q binding sites[57]. Haem detoxification drugs, such as the type 1 quinoline chloroquine and the type 2 quinolines quinine and mefloquine, have a method of action that is still not completely known, but likely involves buildup of

Haem in the parasite food vacuole; resistance is multi-gene and complex in nature[55]. Finally the artemisinin-type compounds are believed to act by oxidative stress, releasing free radicals via a still debated mechanism[58]. Frighteningly, evidence of resistance, particularly along the Cambodia-Thailand border, has been emerging to the artemisinins which are widely considered one of the most powerful weapons against malaria[59].

Summary

Plasmodium falciparum is a disease with an unbalanced burden towards poverty-stricken countries. It remains one of the greatest causes of morbidity and mortality worldwide, particularly in children under five years of age. There remains no vaccine and resistance to existing drug regimens exists and is expanding, with the last major class of antimalarials being introduced more than fifteen years ago[60].

The parasitic life style of *P. falciparum* relies on complicated protein transport machinery to shuttle proteins to specialized organelles, such as the apicoplast[61], and perhaps more intriguingly to export proteins into its host cell, transversing multiple membrane barriers to allow for the remodeling of the infected red blood cell into the ideal living environment[62, 63].

In the past, investigations into protein transport machinery and in particular the secretory pathway have yielded natural molecules that disregulate membrane traffic by enhancing retrograde transport through the endoplasmic reticulum, such as brefeldin A[64], result in Golgi vesiculation by binding Golgi membranes, such as norrisolide[65, 66], or result in Golgi fragmentation, such as macfarlandin E[67]. In addition, novel synthetic small

molecules, such as secramine, have been found to possess the ability to disrupt the secretory pathway[68, 69].

These findings open the door to the discovery of molecular targets for disease, which have already begun to find a place in clinical practice. For example, there have been trials of the mammalian target of rapamycin against breast cancer[70]. The effects of the aforementioned Golgi-disrupting substances on *P. falciparum* have not been closely studied. Yet, libraries of potential drug targets within the secretory pathway of *P. falciparum* exist[60].

Promisingly, the understanding of the protein export continues to improve. For instance, the existence of a translocon to facilitate the export of proteins across the parasitophorous vacuole membrane and the parasite's ability to alter the erythrocyte plasma membrane's permeability by creating new permeation pathways or upregulating existing ion channels[71] reveals hopeful insight. The expansion of knowledge on alternative secretion of proteins, which may be connected to GRASP, could provide answers to the puzzle of PNEP secretion.

A more basic understanding of the secretory pathway, including information on the biogenesis of crucial organelles such as the Golgi apparatus and ERES in *P. falciparum* is lacking. This essential piece of information is the main subject of this thesis. Such knowledge would hopefully translate into the ability to better select drug targets along the secretory pathway, which may lead to new hope in the fight against malaria.

Statement of Purpose

Hypothesis

The Golgi and endoplasmic reticulum exit sites (ERES) in *Plasmodium falciparum*, as visualized by the marker proteins GRASP1, GRASP2 and Sec13p, are formed de novo rather than splitting from existing organelles.

Specific Aims

1. To create and analyze constructs forming *Plasmodium falciparum* parasites that express the fluorescent tags Dendra or GFP attached to the Golgi marker proteins GRASP1 or GRASP2 or the ERES marker protein Sec13p.

2. To examine Golgi and ER exit site biogenesis via time-lapsed 3D confocal microscopy concentrating on signal changes in photobleached or photoconverted *Plasmodium falciparum* parasites expressing the marker proteins GRASP1, GRASP2 or Sec13p along with the fluorescent tags GFP or Dendra

3. To attempt a conditional protein degradation of GRASP1 and GRASP2 utilizing a destabilization domain (DD) and the stabilizing ligand Shld1 in conjuction with the fluorescent tag GFP

Methods

Molecular Cloning of Constructs

The constructs Grasp1pARLDD and Grasp2pARLDD, which were used for attempted conditional protein degradation, were based on the constructs Grasp1pARLGFP and Grasp2pARLGFP (Gilberger lab). Midipreps of Grasp1pARLGFP and Grasp2pARLGFP were each digested with the restriction enzymes AvrII and XhoI for 2 hours at 37ºC in the presence of BSA and NEB Buffer 4 (reagents from New England BioLabs). This created the vectors Grasp1pARL and Grasp2pARL. The destabilization domain (DD) was amplified via polymerase chain reaction (pcr) from a miniprep of DD in the vector pHCAM (Gilberger lab), using the primers DD Sense and DD Antisense (see Table 1). The pcr product was purified with the Macherey-Nagel NucleoSpin Extract II kit and subsequently digested with AvrII and XhoI as detailed above. The digested vectors and the digested insert were again kit-purified and subsequently ligated for 1 hour at room temperature using New England BioLabs T4 DNA Ligase and Ligase Buffer. The ligation products were incubated in electrocompetent XL-Gold *E.Coli* cells (Gilberger Lab), on ice for 20 minutes. The cells were then heat shocked at 42ºC for 30 seconds and immediately placed on ice for 10 minutes. LB was added to each transformation product, which was then incubated at 37ºC, 900 rpm for 45 minutes. The product was then centrifuged at room temperature, 13,200 rpm for 1 minute. The supernatant was discarded and the pellet was smeared onto an LB-Ampicillin plate, which was incubated at 37ºC overnight. Colonies were picked from the plate and screened via colony pcr using the primers DD Sense and DD Antisense to ensure the correct insert (DD) was present.

Selected colonies were grown up in 2mL tubes with LB-Ampicillin overnight. Minipreps were then performed using the Macherey-Nagel Nucleospin Plasmid kit. Miniprep products were subsequently digested with KpnI (restriction site located between the CRT promoter and Grasp1/Grasp2 in the pARL vector) and XhoI at 37ºC for 1 hour in the presence of FastDigest Buffer (reagents from Fermentas). This served as a second check for the presence of the correct insert. Minipreps that were adequately digested were sent for sequencing using DD Sense and DD Antisense Primers (Seqlab Sequence Laboratories Göttingen, Germany). Minipreps showing proper sequences were grown up in 100mL LB-Ampicillin overnight and amplified with the Qiagen Plasmid Midi kit.

The constructs Grasp1pARLGFPDD and GRASP2pARLGFPDD were created with the Grasp1pARL or Grasp2pARL vector, construction described above. The insert, GFPDD, was created by first amplifying GFP using the primers GFP Sense Overlap and GFP Antisense Overlap (Table 1), thereby inserting a 3' PstI restriction site. DD was then amplified using the primers DD Sense Overlap and DD Antisense Overlap (Table 1), which added a 5' PstI site. The two pcr products were mixed and amplified again using the primers GFP Sense Overlap and DD Antisense Overlap to create the final insert, which was subsequently purified and digested with XhoI and AvrII prior to ligation with either vector. Constructs were screened and sequenced as described above.

The constructs Grasp1pARLDendra, GRASP2pARLDendra and Sec13ppARLDendra were created with the vectors Grasp1pARL, Grasp2pARL (construction described above) and Sec13ppARL (Gilberger lab). The insert, Dendra (courtesy of C. Grüring), was amplified via pcr using the primers Dendra Sense and Dendra Antisense (Table 1) and

subsequently purified and digested with XhoI and AvrII prior to ligation with the corresponding vector.

Similarly, the construct Grasp1pARLTapTag was created with the vector Grasp1pARL. The insert, TapTag (Gilberger lab), was amplified via pcr using the primers Tap Sense and Tap Antisense (Table 1) and subsequently purified and digested with XhoI and AvrII prior to ligation with the Grasp1pARL vector.

The construct Grasp1DDpHCAM3xHA was created using the vector pHCAM3xHA (Gilberger lab) digested with the restriction enzymes PstI and NheI (New England BioLabs) at 37°C for 2 hours. The insert, Grasp1(last 1000bp)DD, was amplified via pcr using the construct Grasp1pARLDD, construction detailed above, and the primers Grasp1DD Sense for pH3xHA and Grasp1DD Antisense for pH3xHA (Table 1). The pcr product was subsequently purified and digested with PstI and NheI prior to ligation with the pHCAM3xHA vector.

Plasmodium falciparum Parasite Culture and Transfection

P. falciparum cultures were maintained at 5 % hematocrit in 5mL or 10mL Petri dishes. RPMI-1640 complete medium was used as culture medium. The medium was exchanged every other day. The parasites were cultivated in erythrocytes of blood group 0+ in a gas environment of 5 % O_2, 5 % CO_2 and 90 % N_2 at 37 °C. To estimate culture parasitemia, thin smears were prepared and air dried, followed by fixation in methanol for 1 min and staining in Giemsa solution (1:10 diluted stock solution) for approximately 20 min.

Parasitemia was then estimated using light microscopy. Cultures were diluted when parasitemia reached approximately 10%.

Table 1: DNA primers used in this study. All primers were designed by M. Morales in collaboration with S. Herrmann, unless otherwise noted. Asterisk indicates primers designed by C. Grüring. Restriction enzyme sequences are underlined. Custom DNA oligonucleotides were synthesized by Sigma-Aldrich.

Primer Name	Sequence (5'-3')	Purpose	Restriction Enzyme
DD Sense	GCGCCCTAGGGGAGTGCA GGTGGAAACCATCTCC	Amplify DD for Grasp1pARLDD and Grasp2pARLDD	AvrII
DD Antisense	GCGCCTCGAGTTAATGCATG GCCATGGCCAGGTCCTC	Amplify DD for Grasp1pARLDD and Grasp2pARLDD	XhoI
GFP Sense Overlap	GCGCCCTAGGATGAGTA AAGGAGAAGAACTTTTC	Amplify GFP-DD for Grasp1pARLGFPDD and Grasp2pARLGFPDD	AvrII
GFP Antisense Overlap	GGAGATGGTTTCCACCTGCA CTCCCTGCAGTTTGTATAGT TCATCCATGCC	Amplify GFP-DD to create Grasp1pARLGFPDD and Grasp2pARLGFPDD	PstI
DD Sense Overlap	GGCATGGATGAACTATACA AACTGCAGGGAGTGCAGGT GGAAACCATCTCC	Amplify GFP-DD to create Grasp1pARLGFPDD and Grasp2pARLGFPDD	PstI
DD Antisense Overlap	GCGCCTCGAGTTAATGCAT GGCCATGGCCAGGTCCTC	Amplify GFP-DD to create Grasp1pARLGFPDD and Grasp2pARLGFPDD	XhoI
Dendra Sense*	GCGCCCTAGGATGAAC ACCCCGGGAATTAACC	Amplify Dendra tocreate Grasp1pARLDendra, Grasp2pARLDendra andSec13ppARLDendra	AvrII
Dendra Antisense*	GCGCCTCGAGTTACCAC ACCTGGCTGGGCAGGG	Amplify Dendra to create Grasp1pARLDendra, Grasp2pARLDendra and Sec13ppARLDendra	XhoI
Tap Sense	GCGCCCTAGGTCCATG GAAAAGAGAAGATGG	Amplify TAP Tag to create Grasp1pARLTAPTag	AvrII
Tap Antisense	GCGCCTCGAGTCAGGTTGA CTTCCCCGCGGAATTCGC	Amplify TAP Tag to create Grasp1pARLTAPTag	XhoI
Grasp1DD Sense for PH3xHA	GCGCCTGCAGAAGTGAAT CTAACAATTATAAAAAGG	Amplify Grasp1(last 1000bp)DD to create Grasp1DDpHCAM3xHA	PstI
Grasp1DD Antisense for PH3xHA	GCGCGCTAGCATGCATG GCCATGGCCAGGTCCTC	Amplify Grasp1(last 1000bp)DD to create Grasp1DDpHCAM3xHA	NheI

To transfect constructs into *P. falciparum* parasites, 3D7 wild-type parasites were cultivated to a parasitemia of approximately 10%. Cultures consisting of predominantly young ring stage parasites were synchronized by first centrifuging the culture at 800xg for 5 minutes and discarding the supernatant. The packed red cell pellet was then resuspended in 5% sorbitol in distilled water and incubated at 37°C for 10 minutes. The cells were centrifuged again at 800xg for 5 minutes and washed with RPMI-1640

complete medium. The pellet was then resuspended in 800µL of cytomix (120mM KCl, 0.15mM CaCl, 2mM EGTA, 5mM $MgCl_2$, 10mM K_2HPO_4 and 25mM Hepes, pH 7.6). This was mixed with 100µg of construct plasmid DNA from a midiprep (precipitated with sodium acetate and 100% ethanol) and transferred to an electroporation cuvette. Electroporation was performed using a Bio-Rad gene pulser set at 200Ω. The pulse controls were set to 2.5kV and 25µF with time constants of 0.7-0-9ms. Following electroporation, samples were mixed with 10mL of RPMI-1640 complete medium and placed in a Petri dish. Transfectants were selected using 10nM WR 99210. In addition, constructs containing the destabilization domain (DD) were split following transfection, with half of the culture maintained with Shld1 and the other half without, as a means of control. Culture media and selection agents were changed every day for 10 days following transfection and then every other day. Transfectants were obtained after an average selection period of 5 weeeks.

Frozen stocks of all constructs of *P. falciparum* parasites created were prepared for long term storage. Ring stage cultures with a parasitemia of approximately 10% were subjected to centrifugation at 800xg for 10 minutes. The supernatant was removed and the packed red cells were washed once in RPMI-1640 complete medium. Then 1.5mL of malaria freezing solution (containing 28% glycerol, 3% sorbitol, 0.65% sodium chloride and distilled water) was used to resuspend the pellet. The samples were placed in cryotubes and transferred a liquid nitrogen tank.

Western Blots

Samples of *P. falciparum* cultures were prepared by adding 1mL of 0.1% saponin to cultures with a parasitemia of approximately 10%, followed by centrifugation at 6000rpm for 10 minutes, 3 washes with 1xPBS and resuspension in 1xSDS running buffer (1%SDS, Tris and glycine). Samples were again centrifuged and the supernatant was removed, resulting in a parasite pellet. This was resuspended in 30µL of resuspension buffer and 5µL of reducing dye was added. The sample was heated at 50°C for 10 minutes and centrifuged at 13000rpm for 10 minutes. The supernatant was used for SDS-PAGE, with 7% polyacrylamide gels (Gilberger lab). The proteins were separated for approximately 20 minutes at 120V.

The SDS-PAGE gels containing the proteins of interest were transferred to nitrocellulose membranes (Schleicher & Schüll) using 10 mM CAPS pH 11.2 transfer buffer without methanol and a tankblot device (Bio-Rad). Blocking of free protein was done using 5% milk in 1xPBS for 30 minutes. The primary antibody, rabbit α-*P. falciparum* GRASP (Gilberger lab), was added in a 1:1000 dilution in 5% milk at 4°C overnight. The membrane was then washed twice with 1xPBS. The membrane was blocked with a secondary HRP-coupled sheep α-rabbit antibody (Sigma) in a 1:2500 dilution in 5% milk at room temperature for 2 hours. The membrane was again washed 2 times with 1xPBS and incubated with ECL (GE Healthcare). Chemiluminescent signal was then visualized by exposure of X-ray films.

Chelex PCR

To create the templates for Chelex pcr, 5-10µL of P. falciparum culture with a parasitemia of 10% was obtained and 200µL of chelex resin (Bio-Rad) was added. This

was incubated on a shaker at 60°C, 700rpm for 30 minutes. The sample was then incubated in a hot water bath at 90°C for 10 minutes and then instantly placed on ice for 10 minutes. The sample was centrifuged at 13000rpm for 1 minute. The supernatant was used as the template for pcr, using primers (Table 1) originally used for creation of the construct at interest.

Fluorescence Microscopy and Immunofluorescence Assays

To image the fluorescence in live, unfixed parasites, approximately 50 μL of *P. falciparum* culture was collected from the bottom of culture dishes. If appropriate, this was incubated with 1 μg ml^{-1} DAPI, 4′,6-Diamidine-2′-phenylindole dihydrochloride, (Roche) for 15 minutes at 37°C to image the parasite nucleus. Thin smears on glass slides were then prepared. Images were observed and recorded using a Zeiss Axioscope M1 microscope equipped with a 100×/1,4 oil immersion lens coupled with a Hamamatsu Orca C4742-95 camera and Zeiss Axiovision software.

To perform an immunofluorescence assay, a packed red cell pellet was obtained from *P. falciparum* cultures with a parasitemia of 10%. 1mL of fixing solution (4% formaldehyde, 0.0075% glutaraldehyde, 10xPBS and double distilled water) was added and allowed to incubate for 30 minutes at room temperature. The sample was then centrifuged at 3000rpm for 2 minutes. The supernatant was discarded and the pellet was washed 3 times with 1xPBS. To permeabilize the membrane, the pellet was resuspended in 1mL of 0.1% Triton in PBS, incubated for 10 minutes at room temperature and washed 3 times with PBS. The sample was then blocked with 3% BSA/PBS for 1 hour at room

temperature and then centrifuged at 3000rpm for 2 minutes. The supernatant was discarded and 500µL of the primary antibody (rabbit α-BiP in a 1:2000 dilution, Gilberger lab) was added in 3% BSA/PBS. The sample was incubated at room temperature for 1 hour on a roller and washed 3 times with 1xPBS. The secondary antibody (Alexa-Fluor-594 goat α-rabbit IgG antibody in a 1:2000 dilution, Molecular Probes) was added to samples in aluminium foil-wrapped tubes and incubated for 1 hour on a roller at 4°C. DAPI was then added in a 1:4000 dilution to visualize the nucleus. The sample was washed 3 times for 10 minutes each with 1xPBS. Fluroescence was visualized as described above.

Confocal Microscopy, Photobleaching and Photoconversions

To check fluorescence and obtain 3D reconstruction images and movies, approximately 50µL of live *Plasmodium falciparum* culture was obtained and, if appropriate, incubated with DAPI as described above. Thin smears on glass slides were then prepared. Parasites were imaged at room temperature using an Olympus FV1000 confocal microscope equipped with an Olympus Cellcubator (Olympus). A 100×/1.4 oil immersion lens and Fluoview software v1.7b were used. Cells were viewed using a 488 nm (GFP and DIC) laser lines. Data was analysed and processed using Imaris 6.2.0 Software.

For photobleaching and photoconversions, cells from the parasite culture were arrested on the glass bottom of a sterile, uncoated, hydrophobic 35 mm µ-Dish (Ibidi) using 0.5 mg per ml concanavalin A (Sigma) dissolved in distilled water. Concanavalin A was added to the glass surface for 10 min and washed off using PBS. The *P. falciparum*

culture was resuspended in PBS and allowed to settle on the dish for 5 minutes. PBS was then used to wash off unbound cells and 37 °C phenol red-free culture medium (Gilberger lab) was added to the dish. Cells were viewed using confocal microscopy at 37°C. The multiarea time-lapse function of the Fluoview software and a motorized stage were used to observe multiple areas during each imaging experiment. The Olympus ZDC autofocus system was used to ensure stacks were always imaged at the same position. Image collection parameters were generally a 4 µs dwell time, 16–32 *z*-stacks (0.2–0.4 µm step size), a zoom level of 1–7 and laser levels of 0.1–3% for the 488 nm.

Photobleaching in Sec13pGFP-expressing cells was achieved using the 488nm laser with 85% intensity for a 0.5 second dwell time restricted to the area containing ERES of interest. Generally, cells were subjected to only one beam of photobleaching. Cells were then observed as previously described.

Green to red photoconversion in Sec13pDendra-expressing cells was achieved using 2,000µs dwell time of the 405 nm laser with 0.03% intensity restricted to the area containing ERES of interest. Cells were then observed as previously described.

Results

Analyzing ERES Recruitment

The existing cell line Sec13p-GFP (courtesy of S. Herrmann) was thawed and imaged using fluorescence microscopy to confirm the expected morphology for Sec13p, a COPII vesicle component and ERES marker, was present (Fig 1).

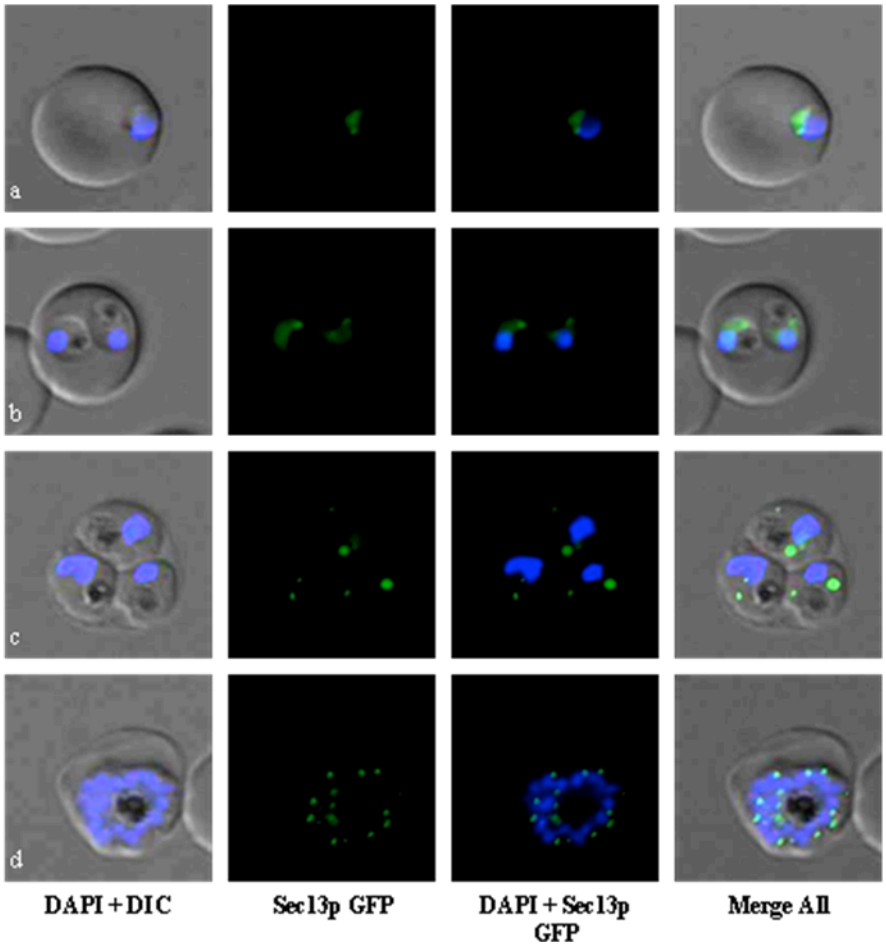

Figure 1. Localization of Sec13p-GFP. Unfixed parasites were stained with DAPI to mark the nucleus and imaged using fluorescence microscopy. There is a single focus of GFP signal, indicating an ERES, in a free merozoite overlying an uninfected RBC (a). Ring form parasites of a doubly infected cell (b) show the GFP focus duplicates prior to nuclear division. As the parasite matures from trophozoite stage (c) to schizont (d) the ERES continue to multiply until each forming merozoite is associated one ERES. Number of iRBCs imaged = 100.

Z-stack images of unfixed Sec13p-GFP parasites in all stages were obtained using confocal microscopy and reconstructed into 3D movies using Imaris software (Fig 2, additional data not shown). These images confirmed fluorescence microscopy images showing Sec13p is tightly compartmentalized near the nucleus. The signal duplicates prior to nuclear division in ring form parasites and continues to multiply until each progeny is associated with one focus of signal, indicating one ERES. No other foci of Sec13p are seen in iRBCs.

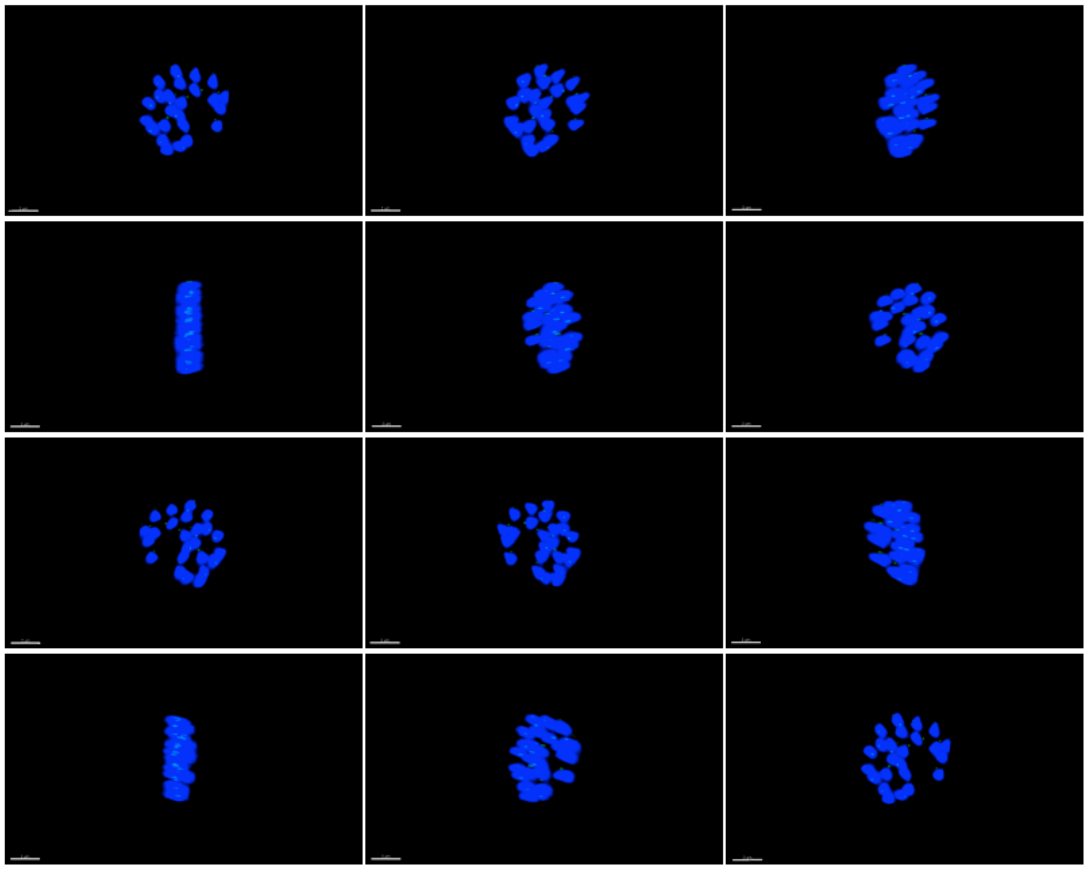

Figure 2. Sec13p-GFP 3D reconstruction. Representative stills from movie showing localization of ERES in three dimensions in a schizont stage parasite. Blue DAPI signal indicates nucleus. GFP signal was noted to be tightly compartmentalized to one ERES per nucleus of the maturing progeny. Size bar indicates 3μm. Number of iRBCs imaged = 20.

After confirming localization of Sec13p-GFP, photobleaching using an argon laser with 488nm illumination was attempted. It was possible to photobleach individual ERES without bleaching neighboring ERES (Fig 3). To ensure the ERES was fully bleached, Z stacks of each parasite were taken to check that signal was eliminated at all 3D levels within the iRBC. All schizont stage parasites photobleached were imaged until the iRBC burst and free merozoites infected a neighboring RBC. This ensured the iRBCs remained viable after photobleaching. The time to GFP signal recovery was found to be 15.2±2.8 seconds (Fig 4). All iRBCs photobleached recovered GFP signal. This information will be utilized further in FLIP (Fluorescence Loss In Photobleaching) and FRAP (Fluorescence Recovery After Photobleaching) experiments in the future.

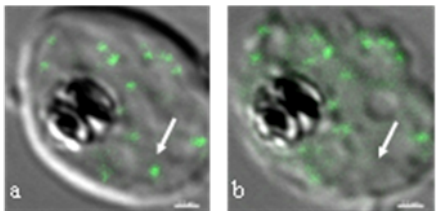

Figure 3. Sec13p-GFP Photobleaching. Representative image from Z stack of an iRBC with GFP signal indicating ERES. White arrow indicates area of isolated ERES prebleach (a) and post bleach (b). Size bar indicates 0.5µm. Number of iRBCs bleached = 20.

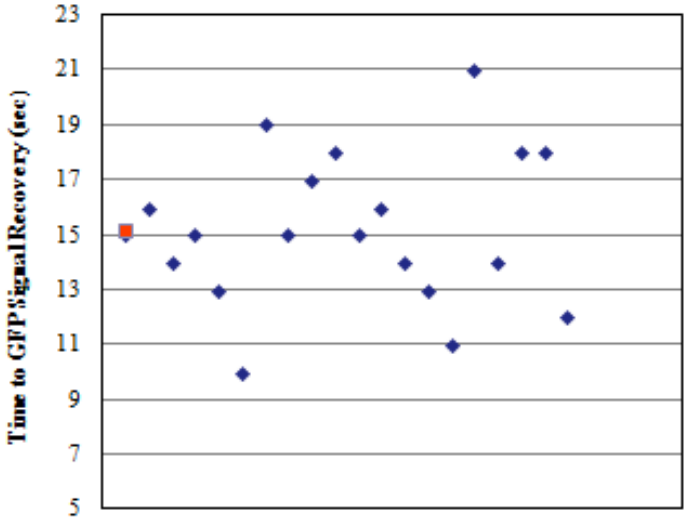

Figure 4. Time to GFP signal recovery in photo-bleached Sec13p-GFP parasites. Each blue dot indicates an iRBC that was photobleached. Red dot indicates mean time to signal recovery of 15.2 seconds with standard deviation of ± 2.8 seconds. Number of iRBCs photo-bleached = 20.

Creating Dendra Constructs

The photobleaching of Sec13p-GFP parasites established that ERES can be individually targeted via confocal microscopy lasers. To further analyze biogenesis of ERES, the cell line Sec13p-Dendra was created. This utilized Dendra2, a green-to-red photoconvertible protein. Sec13p-Dendra demonstrated proper localization to ERES (Fig 5), matching that of Sec13p-GFP. This indicated the Dendra tag did not affect trafficking of Sec13p.

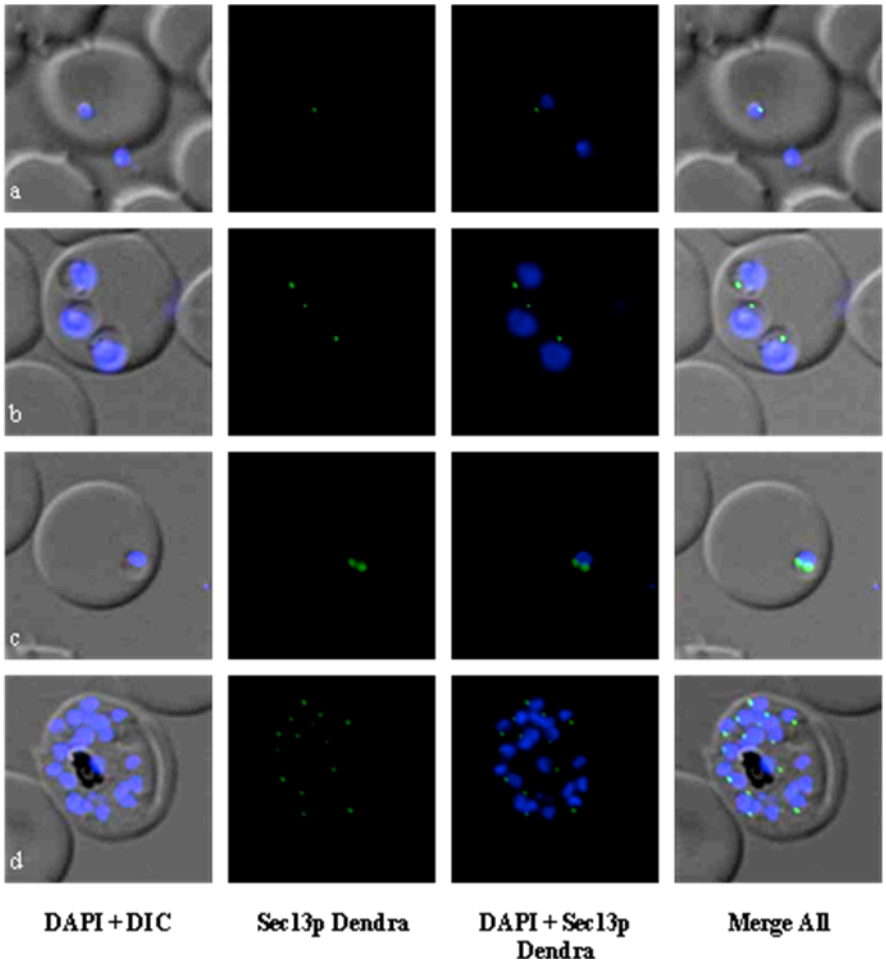

Figure 5. Localization of Sec13p-Dendra. Unfixed parasites were stained with DAPI to mark the nucleus and imaged using fluorescence microscopy. There is a single focus of unconverted Dendra signal, indicating an ERES, in a free merozoite overlying an uninfected RBC (a). Young ring form parasites of a triply infected cell (b) show an identical Dendra focus, which duplicates later in ring stage (c) prior to nuclear division. As the parasite matures into a schizont (d) the ERES continue to multiply until each forming merozoite is associated one ERES. Number of iRBCs imaged = 100.

Since there is no commercially available Sec13p antibody to utilize in western blot confirmation of the construct, further imaging was done to ensure proper positioning of Sec13p-Dendra within the parasite. An immunofluorescence assay with α-BiP, an ER marker, showed Sec13p-Dendra localizes to a tight compartment closely associated with both the nucleus and the ER (Fig 6). This morphology was expected, as it was previously noted for the cell line Sec13p-GFP (data not shown).

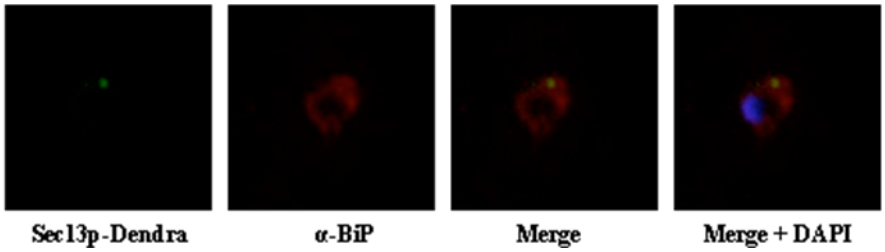

Figure 6. Sec13p-Dendra immunofluorescence assay with α-BiP. Fixed parasites were stained with DAPI to mark the nucleus and imaged using fluorescence microscopy. Unconverted Dendra signal, marking ERES, localizes to a compartment of the cell in close relationship to the nucleus and the ER, marked by α-BiP. Number of cells imaged = 20, experiment repeated 3x.

After the Dendra2 tag was confirmed to have no alteration on Sec13p trafficking throughout the parasite intraerythrocytic cycle, this technology was extended to create two additional cell lines: Grasp1-Dendra and Grasp2-Dendra. These lines would allow for the examination of Golgi biogenesis. Both Grasp1-Dendra (Fig 7) and Grasp2-Dendra (Fig 8) localized to the expected, tightly-defined compartment in close association with the nucleus. The localization pattern is virtually indistinguishable from that of Sec13p. An α-Grasp western blot (Fig 9) confirmed both Grasp1-Dendra and Grasp2-Dendra contained Grasp at the expected size of approximately 70kDa, with Grasp1-Dendra containing two bands secondary to a known splicing event.

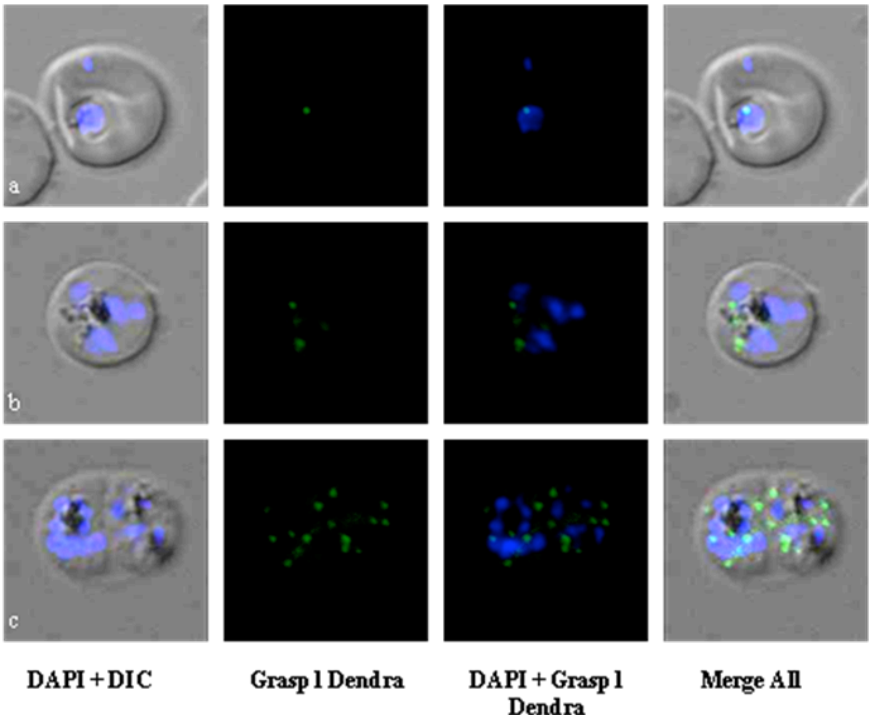

Figure 7. Localization of Grasp1-Dendra. Unfixed parasites were stained with DAPI to mark the nucleus and imaged using fluorescence microscopy. There is a single focus of unconverted Dendra signal, indicating a Golgi, in a young ring stage parasite (a). This focus doubles prior to nuclear division, which takes place in the trophozoite stage (b). As the parasite matures into a schizont (c) the Golgi continue to multiply until each forming merozoite is associated one Golgi. Number of iRBCs imaged = 100.

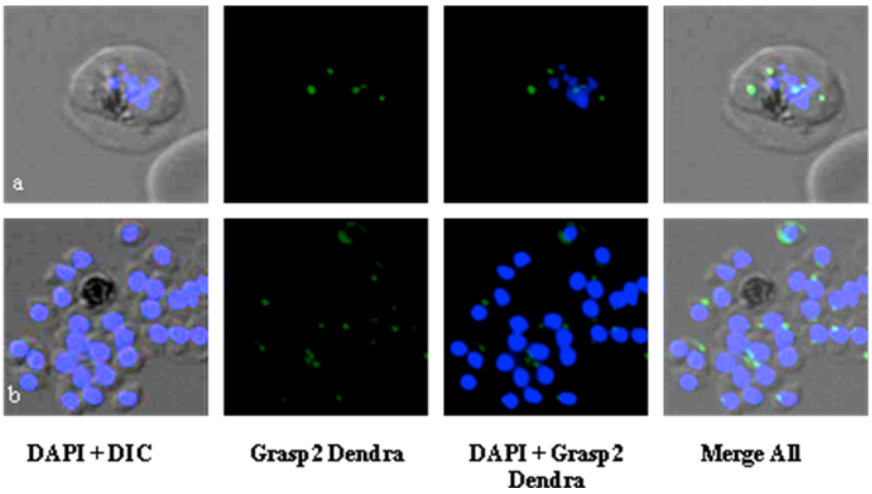

Figure 8. Localization of Grasp2-Dendra. Unfixed parasites were stained with DAPI to mark the nucleus and imaged using fluorescence microscopy. A trophozoite stage parasite (a) shows two foci of unconverted Dendra signal associated with each dividing nucleus. Free merozoites from a recently burst iRBC (b) display one focus of signal, representing a Golgi, associated with each progeny. Number of iRBCs imaged = 100.

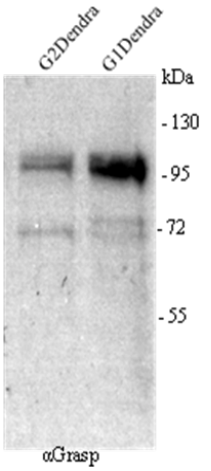

Figure 9. Grasp1-Dendra and Grasp2-Dendra construct confirmation via αGrasp western blot. Lane one (left) shows Grasp2 Dendra containing Grasp at approximately 70kDa. Lane two shows Grasp1 Dendra containing two bands of Grasp, secondary to a known splicing event, at approximately 70kDa. Experiment repeated 3x.

Dendra Photoconversions

After the creation and confirmation of the constructs Sec13p-Dendra, Grasp1-Dendra, and Grasp2-Dendra, photoconversion (an irreversible change from green signal to a stable red signal upon excitation) was attempted with the 405nm laser of a confocal microscope. Unfortunately, the unconverted (green) signal from both Grasp1-Dendra and Grasp2-Dendra were too weak to proceed with photoconversions (data not shown). The signal from Sec13p-Dendra was considerably more intense and photoconversion was possible (Fig 10). Individual ERES could be targeted without affecting neighboring ERES. Full Z stacks of each photobleached parasite were inspected to ensure the ERES was fully converted to red signal in all 3D levels of the iRBC. Schizont stage parasites were followed until iRBCs burst and free merozoites infected neighboring cells, to ensure parasite viability after photoconversion. It was possible to fully photoconvert 20/20 ERES targeted.

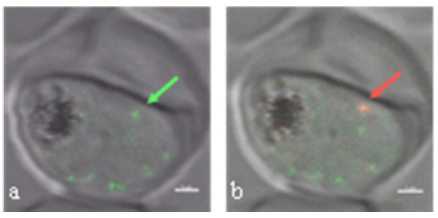

Figure 10. Sec13p-Dendra photoconversion. Representative image from Z stack of an iRBC containing a schizont stage parasite imaged with confocal microscopy pre-conversion (a) and immediately post-conversion (b). Full conversion of the ERES indicated by the green arrow from a green signal to red signal, indicated by red arrow, was possible without affecting surrounding ERES. Size bar indicates 1μm. Number of iRBCs photoconverted = 20.

To better understand ERES biogenesis, ring form parasites were targeted for Sec13p photoconversion, since this is the stage at which ERES are known to duplicate prior to nuclear division. 10 ring form parasites were targeted for photoconversion of the single ERES present (Fig 11). These iRBCs were followed until the formation of a second ERES was seen. In 10/10 parasites, the second ERES was found to contain only unconverted, green Sec13p signal. This indicated the second ERES did not arise from a splitting of the first, which would have resulted in a second ERES containing red, converted Sec13p signal. The evidence suggests the second ERES formed de novo. In zoomed projections of 3D images examining the components of converted and unconverted Sec13p (Fig 12), it is found that new Sec13p is shuttled into the primary ERES by 30 seconds post-photoconversion. This amount of new Sec13p protein increases over time. At the point of new ERES development (Fig 12, 150 seconds post-photoconverison), only green, unconverted signal was observed. Within 30 seconds, red, converted signal was seen within the new ERES. In addition, green, unconverted signal in the old ERES was greatly increased. This is attributed to significant, rapid shuttling of proteins between the two ERES.

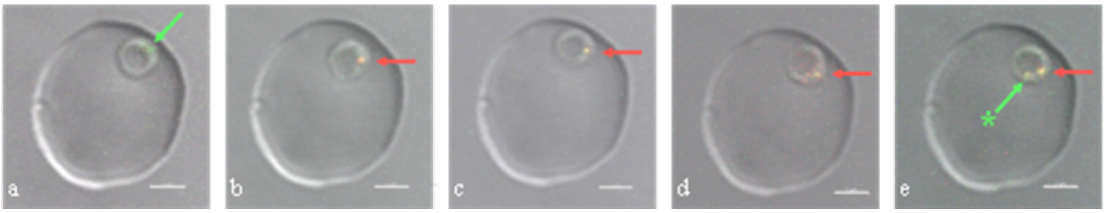

Figure 11. New ERES formation. Representative image from a Z stack of an iRBC containing a young ring form Sec13p-Dendra parasite imaged with confocal microscopy pre-photoconversion (a), immediately post-conversion (b), 30 seconds post-conversion (c), 60 seconds post-conversion (d), and 90 seconds post-conversion (e). A new ERES, indicated by a green arrow (e), was found to have only green, unconverted signal. Size bar indicates 2µm. This phenomenon was visualized in 10/10 ring form parasites photoconverted.

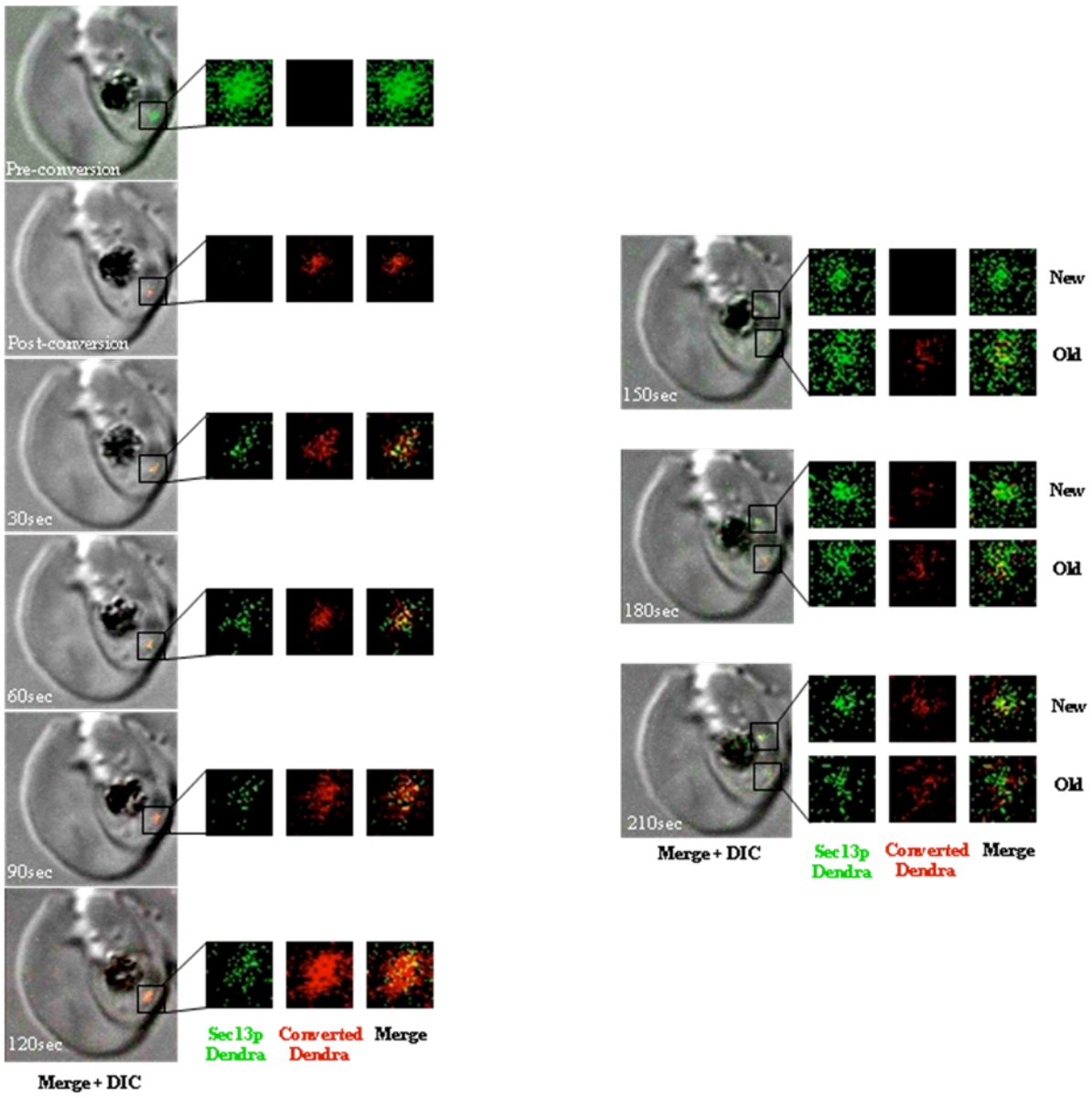

Figure 12. Protein trafficking between ERES. Representative images from Z stacks of a ring form Sec13p-Dendra parasite imaged using confocal microscopy pre-photoconversion, immediately post-photoconversion, and at 30 second intervals thereafter. Boxed insets display zoomed images of 3D projections of Sec13p-Dendra unconverted and converted protein contributing to merged images. At 30 seconds post-conversion, unconverted Dendra signal is visible, indicating new protein being shuttled into the existing ERES. The second ERES, visible at 150 seconds post-conversion displays only unconverted signal, indicating it did not arise from a splitting of the first ERES. By 180 seconds post-conversion, the new ERES displays converted signal, indicating crosstalk from the old ERES. This phenomenon was visible in 10/10 ring form parasites photoconverted.

Investigating GRASP

The previous experiments gathered information on how ERES form. Although ERES biogenesis is closely associated with Golgi biogenesis, it is difficult to draw conclusions on how Golgi form without having a cell line that can be imaged in 4D. Since Grasp1-Dendra and Grasp2-Dendra did not have strong enough signals for photoconversions that could be watched over time, a new approach, involving the conditional degradation of Grasp1 and Grasp 2 was attempted. The constructs Grasp1-DD and Grasp2-DD, along with the similar constructs Grasp1-GFPDD and Grasp2-GFPDD, which utilized a GFP tag for imaging, were created. All four utilized DD, a destabilizing domain, which requires the ligand Shield 1 to allow for stable accumulations of the targeted protein, and results in targeted degradation in its absence. To ensure the DD tag (in the presence of Shield 1) was correctly inserted, Chelex pcr was performed on all four constructs (Fig 13). This technique took purified parasite lysate from each cell line, amplified the insert, and sent the insert for sequencing. After amplification, Grasp1-DD and Grasp2-DD (Fig 13a) were found to have inserts of the expected approximately 350bp, which were confirmed by sequencing to have 100% sequence similarity compared to DD's known sequence. Likewise, amplification of Grasp1-GFPDD and Grasp2-GFPDD (Fig 13b) were found to have inserts of the expected approximately 1050bp, which also had 100% sequence similarity compared to GFPDD's known sequence. The constructs Grasp1-DD and Grasp2-DD were further examined by α-Grasp western blot for the presence of Grasp, to ensure there was no alteration caused by the DD tag in the presence of Shield 1 (Fig 14). The expected Grasp band at approximately 70kDa was seen for both constructs, with an extra band noted for Grasp 1, secondary to a known splicing event.

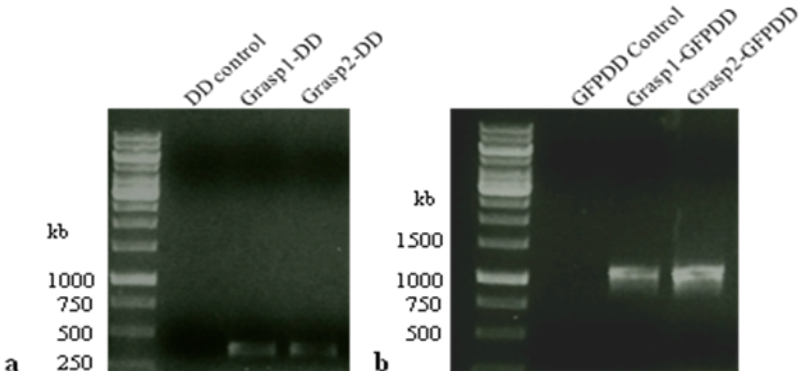

Figure 13. Grasp1/2-DD and Grasp1/2-GFPDD construct confirmation via Chelex PCR. Parasite lysate from the cell lines Grasp1-DD and Grasp 2-DD (a), or Grasp1-GFPDD and Grasp2-GFPDD (b), all cultured in the presence of Shield-1, were prepared for chelex pcr using primers to amplify DD (a) or GFPDD (b). A band of approximately 350kb, corresponding to the size of DD, was seen for both Grasp1-DD and Grasp2-DD (a). A band of approximately 1050kb, corresponding to the size of GFPDD, was seen for both Grasp1-GFPDD and Grasp2-GFPDD (b). Experiment repeated 3x.

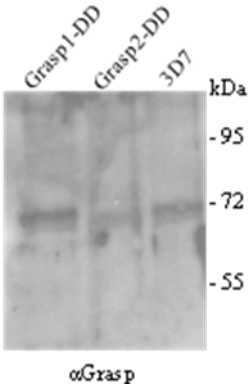

Figure 14. Grasp1-DD and Grasp2-DD construct confirmation via αGrasp western blot. Pellets were prepared from parasites cultured in the presence of Shield-1. Lane one (left) shows Grasp1-DD containing two bands of Grasp, secondary to a known splicing event, at approximately 70kDa. Lane two (middle) shows Grasp2-DD containing Grasp at approximately 70kDa. Lane 3 (right) shows 3D7 WT parasites containing native Grasp at approximately 70kDa. Experiment repeated 3x.

Imaging of the constructs Grasp1-GFPDD and Grasp2-GFPDD were done to check for localization of Grasp (Fig 15). Grasp1-GFPDD was not found to have signal in close association with the nucleus; the signal was still tightly compartmentalized, but improperly targeted. Grasp2-GFPDD was found to have proper signal targeting in close association with the nucleus, however there was a significant portion localizing to the cytoplasm that inhibits further study. In addition, all four lines (Grasp1 or 2-DD and

Grasp1 or 2-GFPDD) were also initially transfected without Shield1, which should have either eliminated Grasp by targeting it for degradation or prevented the parasites from growing altogether, if Grasp was an essential protein. All four cell lines without Shield 1 produced viable parasites, with Grasp still present and microscopic phenotypes for the GFPDD lines identical to those grown in the presence of Shield 1 (data not shown). This was suggestive of improper regulation of the DD system.

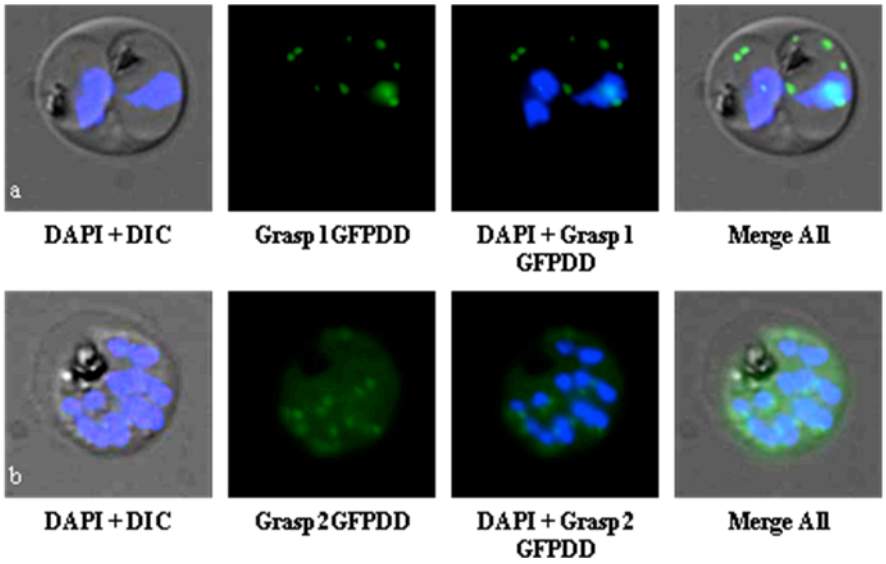

Figure 15. Localization of Grasp1-GFPDD and Grasp2-GFPDD. Unfixed parasites were stained with DAPI to mark the nucleus and imaged using fluorescence microscopy. Grasp1-GFPDD parasites (a) displayed improper targeting, with Golgi signal seen at a distance from the nucleus, in a pattern suggesting Mauer's cleft localization. Grasp2-GFPDD parasites (b) display proper localization with one Golgi signal associated with each forming merozoite in this schizont stage parasite, however a large cytosolic pool is also present. Number of iRBCs imaged = 100.

To further regulate the DD system, a new conditional Grasp knock-out construct was created by inserting the last 1000bp of Grasp1 fused to the DD tag into the pHCAM knock-out vector that allows integration into the parasite DNA via single crossover

recombination (Fig 16a). A triple hemagluttinin tag was added to aid in the purification of GRASP interaction partners. Their subsequent identification will be achieved by mass spectrometry. The proper Grasp1 (last 1000bp)-DD insert of approximately 1300kb was identified following PstI/NheI digestion (Fig 16b). This construct was transfected into parasites and will be analyzed once resistant parasites emerge.

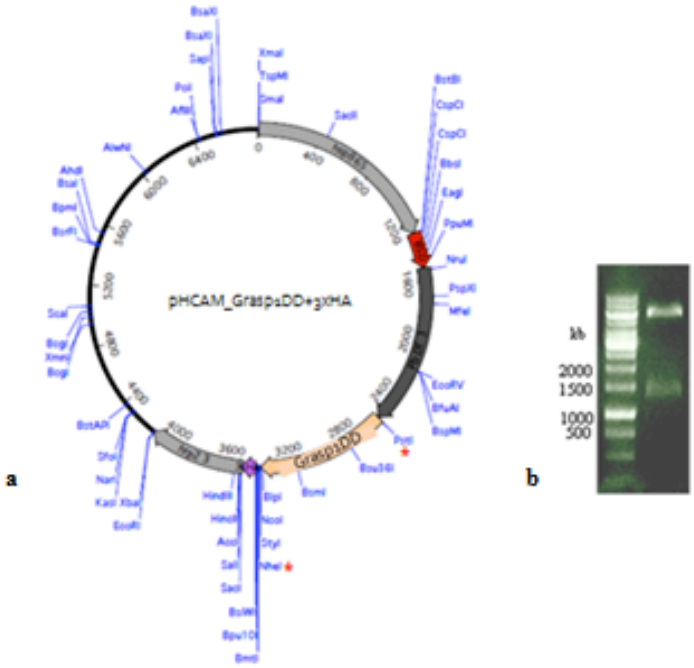

Figure 16. Grasp1 knock-out construction. The last 1000bp of Grasp1 along with the destabilization domain (DD) were cloned into the pHCAM knockout vector (a). The location of Grasp1-DD is indicated by the tan bar, the triple hemagluttinin tag is indicated by the purple bar. The restriction enzymes used for cloning, PstI and NheI, are indicated by red asterisks. Grasp1-DDpHCAM3xHA plasmid confirmation via PstI/NheI digestion is shown in (b). Plasmid DNA was purified and double digested. A band of approximately 1300kb, corresponding to the size of Grasp1(last 1000bp)DD, is visible. An upper band representing the remaining vector is also noted. Experiment repeated 3x.

To analyze Grasp interaction partners via a second approach, Grasp1 was fused to Tap Tag to allow for tandem affinity purification of Grasp and its interaction partners, which could further be investigated by SDS page analysis. An α-Grasp western blot was used to

confirm the presence of Grasp in the construct, seen as a band of approximately 70kDa (Fig 17). Three unknown additional bands of lower sizes were also seen. Tandem affinity purification methods are currently being adjusted to allow for additional product yield prior to SDS page analysis.

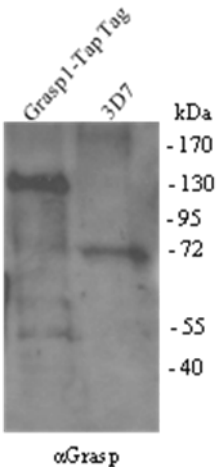

Figure 17. Grasp1-Tap Tag construct confirmation via αGrasp western blot. Lane one (left) shows Grasp1-Tap Tag with a faint band at approximately 70kDa, corresponding to Grasp. This band runs at the same length as the native Grasp band seen in lane two (right), at approximately 70kDa. Source of additional bands is unknown. Experiment repeated 3x.

Discussion

Plasmodium falciparum is the culprit behind the most severe form of human malaria, with over 200 million cases worldwide in 2009[7]. Although the asexual, blood stage of the parasite life cycle causes symptoms of the disease and is the target of nearly all available antimalarials, relatively little is known about the secretory pathway that manages to transport proteins to specialized parasite organelles and also into the host cell, refurbishing the infected red blood cell to the parasite's specifications. This thesis examined the biogenesis of two critical organelles within *P. falciparum*'s secretory pathway: endoplasmic reticulum exit sites (ERES) and the Golgi apparatus. This examination was undertaken via the cloning of parasites containing fluorescently-labeled proteins to identify ERES and the Golgi apparatus, namely Sec13p and GRASP,

respectively. Time lapse 3D microscopy, photobleaching and photoconversions were used to visualize the process. In addition, a more detailed understanding of GRASP in relation to the Golgi was attempted via conditional knock-out of the protein.

ERES Dynamics in Plasmodium falciparum

To visualize ERES in *P. falciparum*, the COPII vesicle component and ERES marker Sec13p was used. The existing parasite line Sec13p-GFP, containing the Sec13p protein fused to a green fluorescent protein reporter was analyzed via fluorescent microscopy and time-lapse 3D confocal microscopy (Figures 1 and 2). As previously reported in the literature[36], a phenotype of one ERES per parasite was seen in early stages, followed by ERES duplication prior to nuclear division. Duplication continued until each forming merozoite was associated with one ERES. In support of previous findings, the ERES were found to be stable and relatively immobile when imaged with time-lapse microscopy[72,73].

To examine recruitment of the protein Sec13p to the ERES, individual ERES were photobleached and the time to maximal fluorescence recovery was recorded (Figures 3 and 4). This technique has previously been employed to examine rhoptry protein trafficking in *P. falciparum*[74]. Time to complete signal recovery was found to be 15.2 ±2.8 seconds. A study performed in vero cells using photobleaching showed the time to half maximal signal recovery for the COPII vesicle components Sar1p, Sec23p, and Sec24p was 1.1sec, 3.7sec, and 3.9 sec respectively; data on Sec13p or time to maximal recovery of signal was not available[75]. The finding for *P. falciparum* Sec13p time to

recruitment is somewhat slower than that study, but may reflect differences in cargo needs of the parasite, which may influence time to COPII vesicle component recruitment. Nevertheless, it is clear that Sec13p is rapidly recruited to ERES in *P. falciparum* and further mathematical analysis of available data with fluorescence recovery after photobleaching and fluorescence loss in photobleaching projections may prove recruitment was faster than first observed.

ERES and Golgi Biogenesis in Plasmodium falciparum

To examine how ERES and the Golgi form in *P. falciparum*, constructs fusing Dendra (a green-to-red photoconvertible protein recently used to examine the Maurer's cleft protein REX2 with time-lapse microscopy in *P. falciparum*[76]) to the protein Sec13p for ERES visualization or GRASP1 or GRASP2 for Golgi visualization were created. The construct Sec13pDendra localized properly and was further confirmed with an α-BiP immunofluorescence assay, showing the relationship between the ER and ERES (Figures 5 and 6). The constructs GRASP1Dendra and GRASP2Dendra also possessed proper localization and were confirmed with α-GRASP western blots (Figures 7, 8 and 9).

However, GRASP1Dendra and GRASP2Dendra displayed a fluorescence signal too weak to be used for time-lapse confocal microscopy and photoconversions. Attempts were made to increase the selection pressure with additional WR 99210 to eliminate any wild-type parasites that may have been present following transfection, however it was not possible to bring fluorescence to the level needed for further direct experiments on Golgi biogenesis. The constructs GRASP1Dendra and GRASP2Dendra have been re-

transfected into wild type parasites and should be re-analyzed for appropriate signal once selection is achieved.

Sec13pDendra did have a strong enough fluorescent signal to continue with photoconversions, and it was possible to fully photoconvert individual ERES from green uncoverted signal to red converted signal in parasites of all stages, in addition neighboring ERES in late-stage parasites were not affected (Figure 10). To ensure full conversion took place, infected red blood cells were imaged in 3D to examine the signal from all angles. Young ring-stage parasites that were followed until duplication of the initial singular ERES was seen were all found to display only green, unconverted signal in the new ERES (Fig 11). This indicates the ERES did not split, which would have resulted in red converted signal or a mix of red and green signal. This is in line with findings seen in *Pichia pastoris* and *Trypanosoma brucei,* where ERES formed de novo and were also associated with the de novo formation of the adjacent Golgi apparatus[43, 44, 77]. Although conclusions on Golgi biogenesis can not be drawn without direct visualization of the apparatus, it can be speculated that Golgi formation closely follows ERES formation in *P. falciparum*, especially due to the close proximity and near identical timing of duplication for ERES and the Golgi within the *P. falciparum* life cycle, shifting the evidence towards likely de novo formation of the Golgi apparatus.

Protein trafficking was also visualized between ERES (Figure 12). Both converted and unconverted Sec13pDendra signal was seen in both ERES as soon as 30 seconds after the formation of the new ERES. This indicates the protein was shuttled between the two locations, possibly to accommodate for extra transport necessary as the cell was about to

undergo nuclear division. Timing of protein transport was in line with that of ERES recruitment seen in previous photobleaching experiments described above.

GRASP Examination in Plasmodium falciparum

The role of GRASP, a Golgi marker known to be anchored to the Golgi membrane and involved in the structural architecture of the organelle[46], is of particular interest in P. falciparum since it possesses two variants of the gene in spite of a simple-appearing, unstacked Golgi[42]. The protein's postulated role in alternative secretion of proteins[50,51] makes it an interesting knock-out candidate to examine the effects on *P. falciparum* Golgi architecture and protein export.

At first, a conditional knock-out of GRASP was attempted by fusing GRASP1 and GRASP2, both with and without a green fluorescent protein reporter to a destabilization domain (DD). This domain was developed as a technique to regulate protein amounts in *P. falciparum*, an organism that lacks RNAi machinery, by allowing stable accumulation of the protein in the presence of the ligand Shld 1 and protein target for destruction in the absence of the ligand[78]. The four constructs GRASP1DD, GRASP2DD, GRASP1GFPDD and GRASP2GFPDD were confirmed with chelex PCR (Figure 13). In addition, GRASP1DD and GRASP2DD were further confirmed with α-GRASP western blots (Figure 14). As a control, parasite transfections were all split into two dishes, one with Shld1 and one without Shld1. All transfectants, with and without Shld1 were viable after selection. However, imaging of parasites containing the GFP reporter (Figure 15) showed improper targeting, resembling that of Maurer's cleft targeting for

GRASP1GFPDD. GRASP2GFPDD showed proper targeting to the Golgi, but the background cytosolic pool of the protein was too great to continue with further imaging or analysis. The presence of viable parasites grown in the absence of Shld1, where GRASP should have been degraded, may indicate GRASP is not essential in *P. falciparum* Golgi formation, given that Golgi were still visualized. However, the lack of a difference in imaging between the groups grown with and without Shld1 likely suggests the DD system was not closely regulated. If proteins were not properly degraded, conclusions on GRASP importance cannot be drawn. Further experiments on DD parameters regulation are currently underway in this laboratory. This may allow more evidence to be gathered once the ideal concentrations of Shld1 in which to grow the parasites and the appropriate timing of Shld1 removal are uncovered.

Meanwhile a more stable method of GRASP degredation was begun, by introducing the last 1000bp of GRASP1, fused to DD into the knock-out vector pHCAM3xHA (Figure 16). This will integrate the insert into the parasite DNA, allowing for a more stable knock-out line, and the presence of a hemagluttinin tag will allow for purification of GRASP interaction partners with subsequent identification via mass spectrometry. These parasites have passed through selection and will be analyzed once the ideal parameters for DD within this laboratory setting are determined. However, if the DD system is not working properly, this construct will also find the issues previously described for the GRASPDD contructs.

Finally, as another method of beginning to examine the interaction partners of GRASP, of particular interest in the realm of alternative secretion of proteins, GRASP1 was fused

to a tandem affinity purification (TAP) tag. The TAP tag consists of ProtA (two IgG binding units for Protein A derived from *Staphylococcus aureus*), TEV (a tobacco etch virus cleavage site) and CBP (a calmodulin binding domain); it is fused to the protein of interest[79]. To analyze the complex, as has been done to identify interaction partners for the *P. falciparum* Translation Elongation Factor complex[80], parasite lysate containing the protein complex is attached to an IgG matrix by the TAP tag ProtA, this is then eluted with TEV protease, incubated with calmodulin-coated beads in the presence of calcium, washed and eluted with EGTA[79]. So far, the desired construct has been created, transfected, selected and confirmed via α-GRASP western blot (Figure 17). The western blot did display additional bands below that expected for GRASP, which could represent some protein degradation or problem with the parasite lysate. Optimization of the purification steps is being done, as product yield was not sufficient in preliminary attempts. A possible issue is the interaction of some endogenous proteins with the CBP portion of the TAP tag, which has been troubleshooted in the past by replacing the CBP with another tag, such as ProtC[79].

Conclusions

In this thesis, it was shown that *Plasmodium falciparum* ERES, as visualized by the COPII vesicle component Sec13p, undergo recruitment at rapid rates of approximately 15.2 seconds following photobleaching experiments. Evidence gathered via time-lapse microscopy in conjunction with photoconversions of Sec13p fused to Dendra showed that ERES form de novo and not by fission. Although conclusive evidence on Golgi biogenesis was not obtained, given the close spatial and duplication time relationship

between ERES and the Golgi in *P. falciparum*, in addition to past studies performed in *P. pastoris* and *T. brucei*, it is speculated that the *P. falciparum* Golgi similarly forms de novo. Strides were made towards the creation of a GRASP knock-out and examination of GRASP interaction partners in *P. falciparum*, which after optimization of methods, may allow for a more detailed study of Golgi biogenesis, GRASP effect on Golgi architecture and on alternative secretion of proteins. The implications of this research are to improve the understanding of the *P. falciparum* secretory pathway, which may lead to easier selection of parasite drug targets in the fight against malaria.

References

1. Cox, F.E.G. 2010. History of the discovery of the malaria parasites and their vectors. *Parasit Vector*. 3:5.
2. Bruce-Chwatt, L.J. 1981. Alphonse Laveran's discovery 100 years ago and today's global fight against malaria. *J R Soc Med.* 74:531-536.
3. Greenwood, B.M., Fidock, D.A., Kyle, D.E., Kappe, S.H.I., Alonso, P.L., et al. 2008. Malaria: progress, perils and prospects for eradication. *JCI.* 118(4):1266-1276.
4. Gething, P.W., Smith, D.L, Patil, A.P., Tatem, A.J., Snow, R.W., et al. 2010. Climate change and the global malaria regression. *Nature.* 465:342-346.
5. Sachs, J. and Malaney, P. 2002. The economic and social burden of malaria. *Nature.* 415:680-685.
6. Teklehaimanat, A. and Paola, M. 2008. Malaria and poverty. *Ann NY Acad Sci.* 1136:32-37.
7. World Health Organization. 2010. Impact of malaria control. *World Malaria Report 2010*. 6:39-61.
8. Limenitakis, J. and Soldati-Favre, D. 2011. Functional genetics in *Apicomplexa*: potentials and limits. *FEBS Letter*s. 585:1579-1588.
9. Rayner, J.C., Liv, M., Peeters, M., Sharp, P.M. and Hahn, B.H. 2011. A plethora of *Plasmodium* species in wild apes: a source of human infection? *Trends Parasitol.* 27(5):222-229.
10. Maguire, J.D. and Baird, J.K. 2010. The 'non-falciparum' malarias: the roles of epidemiology, parasite biology, clinical syndrome, complications and diagnostic rigour in guiding therapeutic strategies. Ann Trop Med Parasitol. 104(4):283-301.

11. Singh, B., Sung, L.K., Matusop, A., Radhakrishnan, A., Shamsul, S.S.G., et al. 2004. A large focus of naturally acquired *Plasmodium knowlesi* infections in human beings. *Lancet.* 363:1017-1024.
12. Richter, J., Franken, G., Mehlhorn, H., Labisch, A. and Häussinger, D. 2010. What is the evidence for the existence of *Plasmodium ovale* hypnozoites? *Parasitol Res.* 107:1285-1290.
13. Wells, T.N.C., Burrows, J.N., Baird, J.K. 2010. Targeting the hypnozoite reservoir of *Plasmodium vivax*: the hidden obstacle to malaria elimination. *Trends Parasitol.* 26(3):145-151.
14. Anstey, N.M., Russell, B., Yeo, T.W., Price, R.N. 2009. The pathophysiology of vivax malaria. *Trends Parasitol.* 25(5):220-227.
15. Tjitra, E., Anstey, N.M., Sugiarto, P., Warikar, N., Kenangalem, E., et al. 2008. Multidrug-resistant *Plasmodium vivax* associated with severe and fatal malaria: a prospective study in Papua, Indonesia. *PLOS Med.* 5(6):890-899.
16. Miller, L.H., Baruch, D.I., Marsh, K. and Doumbo, O.K. 2002. The pathogenic basis of malaria. *Nature.* 415:673-679.
17. Desai, M., Kule, F.O., Nosten, F., McGready, R., Asumoa, K. et al. 2007. Epidemiology and burden of malaria in pregnancy. *Lancet Infect Dis.* 7:93-104.
18. Sturm, A., Amino, R., van de Sand, C., Regen, T., Retclaff, S., et al. 2006. Manipulation of host hepatocytes by the malaria parasite for delivery into liver sinusoids. *Science.* 313:1287-1290.
19. Cowman, A.F. and Crabb, B.S. 2006. Invasion of red blood cells by malaria parasites. *Cell.* 124:755-766.
20. Remarque, E.J., Faber, B.W., Kocken, C.H.M. and Thomas, A.W. 2008. Apical membrane antigen 1: a malaria vaccine candidate in review. *Trends Parasitol.* 24(2):74-84.
21. Waller, K.L., Cooke, B.M., Nunomura, W., Mohandas, N. and Coppel, K.L. 1999. Mapping the binding domains involved in the interaction between the *Plasmodium falciparum* Knob-Associated Histidine-Rich Protein (KAHRP) and the cytoadherence ligand *Plasmodium falciparum* Erythrocyte Membrane Protein 1 (PfEMP1). *JBC.* 274(34):23808-23813.
22. Tilley, L., Sougrat, R., Lithgow, T. and Hanssen, E. 2008. The twists and turns of Maurer's cleft trafficking in *Plasmodium falciparum*-infected erythrocytes. *Traffic.* 9:187-197.
23. Tilley, L., Dixon, M.W.A. and Kirk, K. 2011. The *Plasmodium falciparum*-infected red blood cell. *Int J Biochem Cell Bio.* 43:839-842.
24. Ghosh, S.K., Field, J., Frisardi, M., Rosenthal, B., Mai, Z. et al. 1999. Chitinase secretion by encysting *Entamoeba invadens* and transfected *Entamoeba histolytica* trophozoites: localization of secretory vesicles, endoplasmic reticulum, and Golgi apparatus. *Infect Immun*. 67(6):3073.

25. Dacks, J.B. and Field, M.C. 2007. Evolution of the eukaryotic membrane-trafficking system: origin, tempo and mode. *J Cell Sci*. 120:2977-2985.
26. Rothman, J.E. and Orci, L. 1992. Molecular dissection of the secretory pathway. *Nature*. 355(6359):409-415.
27. Voeltz, G.K., Rolls, M.M., and Rapoport, T.A. 2002. Structural organization of the endoplasmic reticulum. *EMBO Rep*. 3(10):944-950.
28. Shimizu, Y. and Hendershot, L. 2007. Organization of the functions and components of the endoplasmic reticulum. *Adv Exp Med Biol*. 594:37-46.
29. Baumann, O. and Walz, M. 2001. Endoplasmic reticulum of animal cells and its organization into structural and functional domains. *Int Rev Cyt*. 205:149-214.
30. Hammond, A.T. and Glick, B.S. 2000. Dynamics of transitional endoplasmic reticulum sites in vertebrate cells. *Mol Biol Cell*. 11(9):3013-3030.
31. Kuehn, M.J., Herrmann, J.M. and Shekman, R. 1998. COPII-cargo interactions direct protein sorting into endoplasmic reticulum-derived transport vesicles. *Nature*. 391:187-190.
32. Bonifacino, J.S. and Glick, B.S. 2004. The mechanisms of vesicle budding and fusion. *Cell*. 116(2):153-166.
33. Copic, A., Latham, C.F., Horlbeck, M.A., D'Arcangelo, J.G. and Miller, E.A. 2012. ER cargo properties specify a requirement for COPII coat rigidity mediated by Sec13p. *Science*. 335(6074):1359-1362.
34. Adisa, A., Frankland, S., Rug, M., Jackson, K., Maier, A.G. et al. 2007. Re-assessing the locations of components of the classical vessicle-mediated trafficking machinery in transfected *Plasmodium falciparum*. *Int J Parasitol*. 37:1127-1141.
35. Rossanese, O.W., Soderholm, J., Bevis, B.J., Sears, I.B., O'Connor, J. et al. 1999. Golgi structure correlates with transitional endoplasmic reticulum organization in *Pichia pastoris* and *Saccharomyces cerevisiae*. *JCB*. 145(1):69-81.
36. Struck, N.S., Herrmann, S., Schmuck-Barkmann, I., de Souza Dias, S., Haase, S. et al. 2008. Spatial dissection of the cis- and trans-Golgi compartments in the malaria parasite *Plasmodium falciparum*. *Mol Microbiol*. 67(6):1320-1330.
37. Glick, B.S. 2000. Organization of the Golgi apparatus. *Curr Opin Cell Biol*. 12(4):450-456.
38. Mowbrey, K. and Dacks, J.B. 2009. Evolution and diversity of the Golgi body. *FEBS Letters*. 583(23):3738-3745.
39. Gu, F., Crump, C.M. and Thomas, G. 2001. Trans-Golgi network sorting. *Cell Mol Life Sci*. 58(8)1067-1084.
40. De Matteis, M.A. and Luini, A. 2008. Exiting the Golgi complex. *Nature Rev Mol Cell Biol*. 9:273-284.
41. Becker, B. and Melkonian, M. 1996. The secretory pathway of protests: spatial and functional organization and evolution. *Microbiol Rev*. 60(4):697-721.

42. Struck, N.S., Herrmann, S., Langer, C., Krueger, A., Foth, B.J. 2008. *Plasmodium falciparum* possesses two GRASP proteins that are differentially targeted to the Golgi complex via a higher- and lower-eukaryote-like mechanism. *J Cell Sci*. 121(2123-2129).
43. Yelinek, J.T., He, C.Y. and Warren, G. 2009. Ultrastructural study of Golgi duplication in *Trypanosoma brucei*. *Traffic*. 10(3):300-306.
44. He, C.Y. 2007. Golgi biogenesis in simple eukaryotes. *Cell Microbiol*. 9(3):566-572.
45. Pelletier, L., Stern, C.A., Pypaert, M., Sheff, D., and Ngo, H.M. 2002. Golgi biogenesis in *Toxoplasma gondii*. *Nature*. 418:548-552.
46. Barinaga-Rementeia Ramirez, I. And Lowe, M. 2009. Golgins and GRASPs: holding the Golgi together. *Sem Cell Dev Biol*. 20(7):770-779.
47. Shorter, J., Watson, R., Giannakou, M.-E., Clarke, M., Warren, G. et al. 1999. GRASP55, a second mammalian GRASP protein involved in the stacking of Golgi cisternae in a cell-free system. *EMBO J*. 18:4949-4960.
48. Wang, Y., Saton, A. and Warren, G. 2005. Mapping the functional domains of the Golgi stacking factor GRASP65. *JBC*. 280(6):4921-4928.
49. Vinke, F.P., Grieve, A.G. and Rabouille, C. 2011. The multiple facets of the Golgi reassembly and stacking proteins. *Biochem J*. 433:423-433.
50. Kinseth, M.A., Anjard, C., Fuller, D., Guiyyunti, G., Loomish, W.F. et al. 2007. The Golgi-associated protein GRASP is required for unconventional protein secretion during development. *Cell*. 130(3):407-409.
51. Levi, S.K. and Glick, B.S. 2007. Grasping unconventional secretion. *Cell*. 130(3):407-409.
52. Manjithaya, R., Anjard, C. Loomis, W.F. and Subramani, S. 2010. Unconventional secretion of *Pichia Pastoris* Acb1 is dependent on GRASP protein, peroxismal functions and autophagosome formation. *JCB*. 188(4):537-546.
53. Haase, S. and de Koning-Ward, T.F. 2010. New insights into protein export in malaria parasites. *Cell Microbiol*. 12(5):580-587.
54. Spielmann, T. and Gilberger, T.-W. 2010. Protein export in the malaria parasite: do multiple export motifs add up to multiple export pathways? *Trends Parasitol*. 26(1):6-10.
55. Olliaro, P. 2001. Mode of action and mechanisms of resistance for antimalarial drugs. *Pharmacol Therapeut*. 89:207-219.
56. Gregson, A. and Plowe, C.V. 2005. Mechanisms of resistance of malaria parasites to antifolates. *Pharmacol Rev*. 57(1):117-145.
57. Srivasta, K. and Vaidy, A.B. 1999. A mechanism for the synergistic antimalarial action of atovaquone and proguanil. *Antimicrob Agents Chemother*. 43:1334-1339.
58. Meshnick, S.R. 2002. Artemesinin: mechanisms of action, resistance and toxicity. *Int J Parasitol*. 32(13)1655-1660.

59. Dondorp, A.M., Yeung, S., White, L., Nguon, C., Day, N.P.J. et al. 2010. Artemisinin resistance: current status and scenarios for containment. *Nat Rev Microbiol*. 8:272-280.
60. Gamo, F.-J., Sanz, L.M., Vidal, J., de Cozar, C., Alvarez, E., et al. 2010. Thousands of chemical starting points for antimalarial lead identification. *Nature*. 465:305-310.
61. Tonkin, C.J., Kalanon, M. and McFadden, G.I. 2008. Protein targeting to the malaria parasite plastid. *Traffic*. 9:166-175.
62. Marti, M., Good, R.T., Rug, M., Knuepfer, E. and Cowman, A.F. 2004. Targeting malaria virulence and remodeling proteins to the host erythrocyte. *Science*. 306(5703):1930-1933.
63. Hiller, N.L., Bhattacharjee, S., van Ooij, C., Liolios, K., Harrison, T. et al. 2004. A host-targeting signal in virulence proteins reveals a secretome in malarial infection. *Science*. 306(5703):1934-1937.
64. Klausner, R.D., Donaldson, J.G. and Lippicott-Schwarz, J. 1992. Brefeldin A: Insights into the control of membrane traffic and organelle structure. *JCB*. 116(5):1071-1080.
65. Brady, T.D., Wallace, E.K., Kim, S.H., Guiyyunti, G., Malhotra, V. et al. 2004. Fragmentation of Golgi membranes by norrisolide and designed analogues. *Bioorg Med Chem Lett*. 14(20):5035-5039.
66. Guizzunti, G., Brady, T.P., Malhotra, V. and Theodorakis, E.A. 2006. Chemical analyis of norrisolide-induced Golgi vesiculation. *J Am Chem Soc*. 128:4190-4191.
67. Schnermann, M.J., Beaudry, C.M., Egorova, A.V., Polishchuck, R.S., Sütterlin, C et al. 2010. Golgi-modifying properties of macfarlandin E and the synthesis and evaluation of its 2,7-dioxabicyclo [3.2.1] octan-3-one core. *PNAS*. 107(14):6158-6163.
68. Pelish, H.E., Westwood, N.J., Fen, Y., Kichhause, T. and Shair, M.D. 2001. Use of biomimetic diversity-oriented synthesis to discover galantamine-like molecules with biological properties beyond those of the natural product. *J Am Chem Soc*. 123:6740-6741.
69. Pelish, H.E., Peterson, J.R., Salvareyya, S.B., Rodriguey-Boulan, E., Chen, J.-L. et al. 2006. Secramine inhibits Cdc42-dependent functions in cells and Cdc42 activation in vivo. *Nat Chem Biol*. 2(1):39-46.
70. Mita, M.M., Mita, A. and Rowinsky, E.K. 2003. Mammalian target of rapamycin: a new molecular target for breast cancer. *Clin Breast Ca*. 4(2):126-137.
71. Merckx, A., Nivey, M.-P., Bouyer, G., Alano, P., Langsley, G. et al. 2008. *Plasmodium falciparum* regulating subunit of cAMP-dependant PKA and anion channel conductance. *Plos Pathog*. 4(2):1-11.
72. Budnik, A. and Stephens, D.J. 2009. ER exit sites – localization and control of COPII vesicle formation. *FEBS Letters*. 583(23):3796-3803.

73. Stephens, D.J., Lin-Marq, N., Pagano, A., Pepperkok, R. and Paccard, J.P. 2000. COPI coated ER to Golgi transport complexes segregate from COPII in close proximity to the ER. *J Cell Sci*. 113:2172-2185.
74. Layez, C. Nagueira, P., Combes, V., Costa, F.T.M., Juhan-Vague, I. et al. 2005. *Plasmodium falciparum* rhoptry protein RSP2 triggers destruction of the erythroid lineage. *Blood* 106:3632-3638.
75. Forster, R., Weiss, M., Zimmerman, T., Reynaud, E.G., Verissimo, F. et al. 2006. Secretory cargo regulates turnover of COPII subunits at single ER exit sites. *Curr Biol*. 16(2):173-179.
76. Grüring, C., Heiber, A., Kruse, F., Ungefehr, J., Gilberger, T.W. et al. 2011. Development and host cell modifications of *Plasmodium falciparum* blood stages in four dimensions. *Nature Comm*. 2(165).
77. Bevis, B.J., Hammond, A.T., Reinke, C.A. and Glick, B.S. 2002. De novo formation of transitional ER sites and Golgi structures in *Pichia pastoris*. *Nature Cell Biol*. 4(10):750-756.
78. Armstrong, C.M. and Goldberg, D.E. 2007. An FKBP destabilization domain modulates protein levels in *Plasmodium falciparum*. *Nature Methods*. 4:1007-1009.
79. Xu, X., Song, Y, Li, Y., Chang, J. Yhang, H. et al. 2010. The tandem affinity purification method: an efficient system for protein complex purification and protein interaction identification. *Protein Expres Purif*. 72(2):149-156.
80. Takebe, S., Witola, W.H., Schimanski, B., Günzl, A., Ben Mamoun, C. 2007. Purification of components of the translation elongation factor complex of Plasmodium falciparum by tandem affinity purification. Euk Cell. 6(4):584-591.